# RESEARCH ACTIVITIES IV
# Department of Molecular Assemblies

## IV-A Optical Study of Charge Ordering States in Organic Conductors

In the organic charge-transfer salts, the charge carriers in organic crystal is located at the boundary between localized and extended (delocalized) states, mainly because the interatomic distances between the neighboring molecules are much longer than the bond length within the molecule. Therefore, charge ordering (CO) originated from the localization of the charge carriers is widely found in organic conductors through the phase transition. Recently, CO has been found in several organic conductors, and the electronic phase diagrams of typical organic conductors are re-considered taking CO into account. The CO state is drawing attention, first because a CO phase is neighbored on a superconducting phase, wherein a new type of pairing mechanism for superconductivity is theoretically predicted, second because some compounds in a CO phase shows ferroelectricity, the origin of which is expected to be electronic, third because the narrow-band compounds have an unusual intermediate state between metallic and CO state. To detect CO states, we employ infrared and Raman spectroscopy. Some molecules have charge-sensitive intramolecular vibrational modes, the frequency of which shifts depending upon the molecular charge (oxidation state of molecule). The Raman and infrared spectra change dramatically at the CO phase-transition temperature, since CO is accompanied by an inhomogeneous distribution with large amplitude. The goal of this study is (1) the understanding of the intermediate state above the CO phase transition, (2) the investigation of the optical properties related to the ferroelectric CO phase, and (3) the characterization of the insulating electronic state near the superconducting phase.

### IV-A-1 Charge Ordering State of β”-$(ET)_3(HSO_4)_2$ and β”-$(ET)_3(ClO_4)_2$ by Temperature-Dependent Infrared and Raman Spectroscopy

**YAMAMOTO, Takashi; URUICHI, Mikio; YAKUSHI, Kyuya; KAWAMOTO, Atsushi[1]**
*([1]Hokkaido Univ.)*

[*Phys. Rev. B* **73**, 125116 (12 pages) (2006)]

We present the temperature-dependent infrared and Raman spectra of β”-$(ET)_3X_2$ (X = $HSO_4$ and $ClO_4$; ET = Bis-ethylenedithio-tetrathiafulvalene) compounds which undergo a metal-insulator transition. The infrared-active $\nu_{27}$ mode discontinuously split into two bands at the metal–insulator transition temperature of 127 K in the X = $HSO_4$ salt, whereas, the corresponding mode continuously changed across the metal–insulator transition temperature of ~170 K in the X = $ClO_4$ salt. In both compounds, the charge-sensitive $\nu_{27}$ mode split into two in the insulating phase. This drastic spectral change indicates that the metal–insulator transition originated in the charge ordering. Employing the frequencies of the split $\nu_{27}$ bands, the site charges are estimated to be $+0.3_4$ and $+0.8_1$ for X = $HSO_4$ and $+0.3_6$ and $+0.8_1$ for X = $ClO_4$. We also estimated the site charges using the Raman-active $\nu_2$ mode and obtained consistent results. Examining the selection rule of the $\nu_3$ mode, we reached the conclusion that the unit cell with space group *P*1 has a pseudo-inversion center in the charge-ordered phase. Based on the symmetry, we propose a charge-ordering pattern for the X = $HSO_4$ and X = $ClO_4$ salts, which is quite different from that of the X = $ReO_4$ salt reported previously. We qualitatively discuss the differences in the charge-ordering pattern considering the anisotropic inter-site Coulomb interaction.

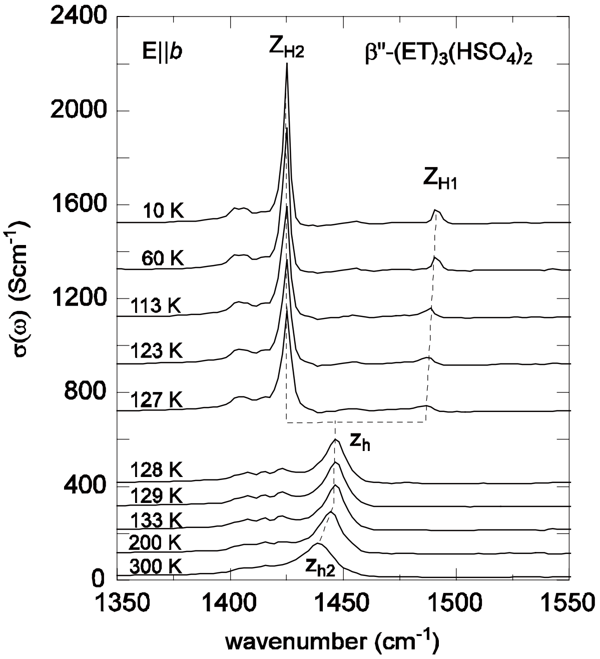

**Figure 1.** Temperature dependence of the conductivity spectra obtained through Kramers-Kronig transformations of the *b*-polarized reflectance spectra of β”-$(ET)_3(HSO_4)_2$. The infra-red-active bands, $z_h$ is the out-of-phase mode of the ring C=C stretching in highly conductive phase. The bands, denoted by $Z_{H1}$ and $Z_{H2}$ are respectively the ring C=C stretching modes of charge-poor and charge-rich molecules of β”-$(ET)_3(HSO_4)_2$.

## IV-A-2 Infrared and Raman Studies of the Charge-Ordering Phase Transition at ~170 K in the Quarter-Filled Organic Conductor, β”-(ET)(TCNQ)

**URUICHI, Mikio; YAKUSHI, Kyuya; YAMAMOTO, Hiroshi M.[1]; KATO, Reizo[1]**
*([1]RIKEN and JST/CREST)*

[*J. Phys. Soc. Jpn.* **75**, 074720 (2006)]

We present the optical conductivity, infrared- and Raman-active charge-sensitive phonon modes, and the x-ray diffraction superlattice spots of β”-(ET)(TCNQ) [ET = bis(ethylenedithio) tetrathiafulvalene, TCNQ = 7,7,8,8-tetracyanoquino-dimethane], which is characterized as a quarter-filled narrow band system. Above ~170 K, we found weak superlattice spots and splitting of the C=C and C–S stretching modes of ET. These results indicate the charge-ordering state in the ET layer. As the temperature is decreased, the superlattice spots abruptly disappeared at ~170 K and the split modes continuously merged into a single band below ~170 K. Concomitantly, the spectral weight of the optical conductivity ascribed to the ET layer significantly shifts toward lower energy. Through the analyses of these experimental results, we propose the view that the incoherent conducting electron in the ET layer shows a crossover behavior into a coherent Fermi liquid state below the structural phase transition at ~170 K.

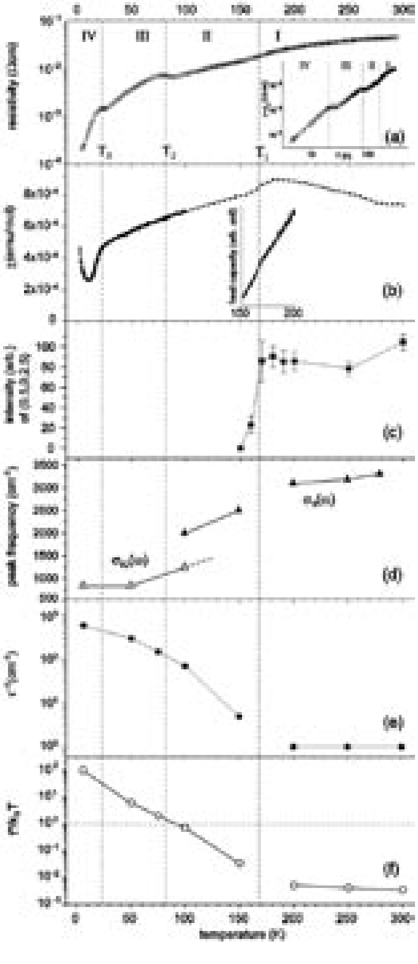

**Figure 1.** Comparison of (a) the dc resistivity, (b) the magnetic susceptibility and heat capacity (inset), (c) the intensity of the superlattice (1/2, 0, 21/2), (d) peak frequency in the optical conductivity of ET layer, (e) the intersite hopping rate in the ET layer, (f) the ratio of effective transfer energy to temperature.

## IV-A-3 Unusual Intermediate State between Metallic and Charge-Ordered States in θ-Type ET Salts

**TAKAHASHI, Toshihiro[1]; NOGAMI, Yoshio[2]; YAKUSHI, Kyuya**
*([1]Gakushuin Univ.; [2]Okayama Univ.)*

[*J. Phys. Soc. Jpn.* **75**, 051008 (2006)]

The Raman spectrum of narrow-band θ-type ET salts in highly conducting phase exhibit a single broad band as shown in Figure 1(c). This Raman band was assigned to the $\nu_2$ mode based on the isotope shift of the $^{13}$C-substituted compound. If the high-temperature phase is a metal, the $\nu_2$ mode should appear between the $\nu_{2P}$ and $\nu_{2R}$ bands which are shown in Figure 1(a). However, the broad $\nu_2$ band above $T_{CO}$ is located at the $\nu_{2R}$ band. In addition, the $\nu_{2P}$ mode, the counterpart of $\nu_{2R}$, is found in the highly conducting phase of the monoclinic TlZn salt (See Figure 1(b)). These spectra were quite different from the spectrum (Figure 1(d)) of metallic θ-$(ET)_2I_3$, in which the $\nu_2$ mode nearly located at the center of $\nu_{2P}$ and $\nu_{2R}$ modes. The spectra of the narrow-band compounds in high-temperature phase rather resemble the spectrum (Figure 1(a)) of charge-ordered state. Therefore, the charges in high-temperature phase are nearly localized and hop to neighbor site slowly less than $10^{11}$ Hz (~1 meV). This hopping rate is much slower than the motion of the charge carriers of organic metal. The high-temperature phase of narrow-band θ-type ET salts is considered as an intermediate state between metallic and CO states.

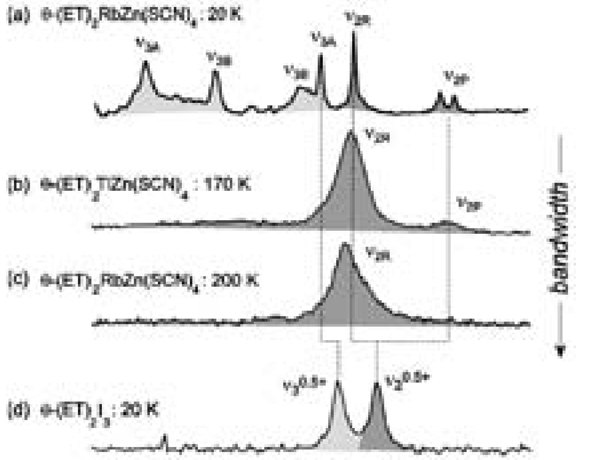

**Figure 1.** Comparison of the $\nu_2$ and $\nu_3$ bands of (a) the CO phase of RbZn, high-temperature phases of (b) TlZn, (c) RbZn, and (e) $I_3$ salts. Note that the $\nu_2$ mode in high-temperature phase of (b) and (c) is already split.

### IV-A-4 Photo-Gatable Second Harmonic Generation in Ferroelectric Organic Conductor with Strongly Correlated Electrons

**YAMAMOTO, Kaoru; IWAI, Shinichiro[1,2]; BOYKO, Sergiy[3]; KASHIWAZAKI, Akimitsu[1]; HIRAMATSU, Fukiko[1]; OKABE, Chie; NISHI, Nobuyuki; YAKUSHI, Kyuya**
*([1]Tohoku Univ.; [2]JST/PREST; [3]Univ. Ontario)*

Ferroelectricity is characterised by the spontaneous polarisation, which shows dramatic temperature- and electric-field responses. By means of optical second-harmonic generation (SHG) measurement, we demonstrated that a two-dimensional organic metal $\alpha$-$(ET)_2I_3$ [ET: bis(ethylenedithio)tetrathiafulvalene] undergoes ferroelectric transformation associated with Wigner-crystal like charge ordering (CO). It was found that the nonlinear electric susceptibility of the compound in the ferroelectric state was much greater than that of a nonlinear optical crystal $\beta$-$BaB_2O_4$ (BBO), suggesting the generation of macroscopic polarisation as in ferroelectrics. In terms of controlling the electronically induced FE polarisation, the photo-response of the macroscopic polarisation to femtosecond laser pulse was investigated. Pump-probe SHG measurement showed that the polarisation was sharply suppressed by the photo-excitation. More noteworthy is the fact that the suppressed polarisation instantaneously recovered in the time scale of 10 ps. The photo-gatable optical nonlinearity based on the electron FE might be applied as a unique medium that functions as a fast optical switch in future all-optical devices.

### IV-A-5 Evaluation of Charge Transfer Degree in the Bis(ethylenethio) Tetrathiafulvalene Salts by Raman Spectroscopy

**KOWALSKA, Aneta[1]; WOJCIECHOWSKI, Roman[1]; ULANSKI, Jacek[1]; MAS-TORRENT, Marta[2]; LAUKHINA, Elena[2]; ROVIRA, Concepcio[2]; YAKUSHI, Kyuya**
*([1]Univ. Lodz; [2]Inst. Ciencia Mater. Barcelona)*

[*Synth. Met.* **156**, 75 (2006)]

Raman spectroscopy studies for a series of charge-transfer salts based on the bis(ethylenethio)tetrathiafulvalene (BET-TTF) were carried out in order to analyze the charge distribution on the donor molecules in the unit cell of crystals. With the help of the density functional theory calculations for $BET\text{-}TTF^0$ and $BET\text{-}TTF^+$ molecules it was shown that the Raman spectroscopy can be applied to determine the stoichiometry in the BET-TTF salts. For salts exhibiting increase of the resistivity below *ca.* 100 K, the Raman spectra at variable temperature indicate that this behavior is not related to the charge disproportionation phenomenon.

### IV-A-6 Installation of a Cryostat to the Far-Infrared Spectrometer and the Transmission Measurement of $\alpha$-(BEDT-TTF)$_2$I$_3$

**YAKUSHI, Kyuya; YAMAMOTO, Kaoru; NAKANO, Chikako**

The measurement of the reflectivity or transmittance in the far-infrared region of organic conductors has been conducted for very restricted materials, owing to the difficulty of the growth of a large single crystal of several mm. The optical conductivity in the far-infrared region provides the information of the electronic state near Fermi energy. For example, the incoherent conducting state is expected to give a non-Drude type optical conductivity, whereas the coherent state provides a well-defined Drude type conductivity. The absorption spectrum of insulating compounds provides the information of the low-frequency local phonons and lattice phonons, which are sometimes closely related to the mechanism of phase transition. We have installed a top-loading type of cryostat, Oxford Optistat CF, to the far-infrared spectrometer, Bruker IFS-66v, whose sample and optics chamber can be evacuated to avoid the strong absorption of water vapor. We introduced a XY stage to fix the bottom of the cryostat to adjust the sample position. Z position can be adjusted using a sample rod controlled by a micrometer. Figure 1 shows the polarized transmittance spectrum of $\alpha$-(BEDT-TTF)$_2$I$_3$ of 2 mm × 2 mm. As shown in this figure, the optical gap appears abruptly at 136 K. Although this phase transition is of first order, the evolution of the gap was observed. This observation is consistent with the evolution of the SHG (second harmonic generation) signal below the phase transition temperature.

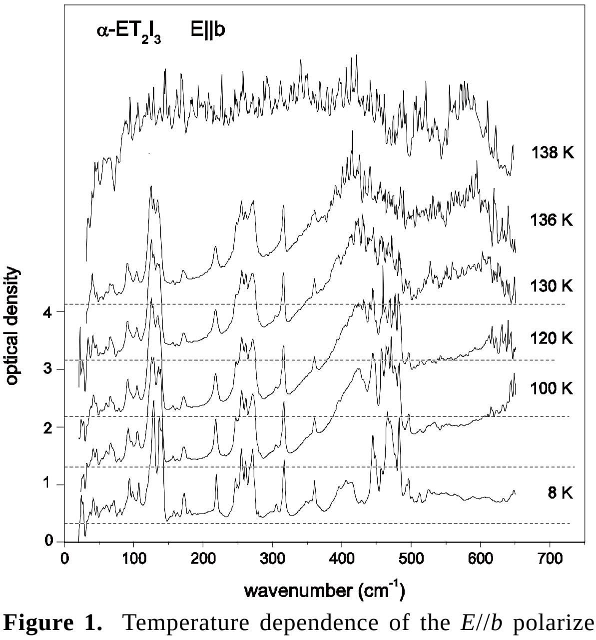

**Figure 1.** Temperature dependence of the *E*//*b* polarized transmittance of the single crystal of $\alpha$-(BEDT-TTF)$_2$I$_3$. Note that the evolution of the gap is observed.

### IV-A-7 Mechanism of the Phase Separation in the Monovalent-to-Divalent Phase Transition of Biferrocenium-(F$_1$TCNQ)$_3$

**URUICHI, Mikio; YAKUSHI, Kyuya; MOCHIDA, Tomoyuki[1]**
*([1]Toho Univ.)*

The ionic crystal $D^+A_3^-$ (D = dineopentylbiferrocene and A = $F_1$TCNQ) undergoes a first-order phase transition, in which second ionization occurs to form a doubly ionized state, $D^{2+}A_3^{2-}$.1) This monovalent-to-divalent phase transition continuously occurs in a wide temperature range from 160 K to 100 K. X-ray diffraction and Raman spectroscopy showed that the macroscopic domains of monovalent and divalent phases coexist in this temperature range.2) We investigated this unusual phase transition and elucidated the mechanism of the phase separation based on the general understanding of the first-order phase transition. According to the theory of first-order phase transition, the free-energy *vs.* order parameter has an energy barrier $E_B$ between the two phases (monovalent and divalent phases). (See Figure 1) If $E_B$ is smaller than the phase transition temperature $kT$ ($T$ ~ 100–160 K), one of the domains can be thermally activated. Therefore, the continuous phase change accompanied by the phase separation can be well explained. Interestingly, the behavior of the first-order phase transition changes from hysteretic behavior to continuous behavior on decreasing the ratio $kT/E_B$ as shown in Figure 1. We speculate that the small energy barrier arises from the mechanism of this phase transition that the Madelung energy gain is the driving force.

**References**

1) T. Mochida, K. Takazawa, M. Takahashi, M. Takeda, Y. Nishio, M. Sato, K. Kajita, H. Mori, M. M. Matsushita and T. Sugawara, *J. Phys. Soc. Jpn.* **74**, 2214 (2005).
2) M. Uruichi, K. Yakushi and T. Mochida, *J. Low Temp. Phys.* in press.

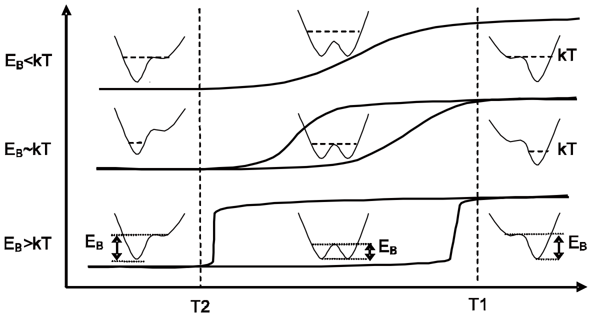

**Figure 1.** The behavior of first-order phase transition is classified by the ratio between the energy barrier $E_B$ and the phase transition temperature $kT$. Abscissa is temperature and ordinate is the physical quantity that changes through a phase transition.

# IV-B Magnetic Resonance Studies for Molecular-Based Conductors

Magnetic resonance measurements may be mature techniques as devices of the so-called chemical analyses. However, from the viewpoint of the solid state material science, magnetic resonance measurement is challenging area still in under the special condition such cases as the extreme low temperature, strong magnetic field, high pressure, electric field, optical response and so on. Moreover they are advantageous for studying the fundamental electronic properties and for understanding the detailed electronic structures of molecular based compounds. Molecular based conductors are one of the extensively studied materials. The development of the understanding of the electronic phases of these materials enables us systematic investigations of low-dimensional highly correlated electrons systems. Competition of the electronic phases in molecular based conductors has attracted much attention. The investigations of such electronic phases by means of magnetic resonance measurements are important to understand the unsolved fundamental problems in the field of solid state physics.

In this project, we performed the multi-frequency- (X-, Q- and W-bands) and pulsed-ESR, and broad-line NMR measurements for molecular based conductors to understand the electron spin dynamics in the low temperature electronic phases.

## IV-B-1 Deuteration Effect and Possible Origin of the Charge-Ordering Transition of (TMTTF)$_2$*X*

**FURUKAWA, Ko; HARA, Toshifumi; NAKAMURA, Toshikazu**

[*J. Phys. Soc. Jpn.* **74**, 3288–3294 (2005)]

ESR, NMR and X-ray measurements were performed for pristine and fully perdeuterio-TMTTF, TMTTF-$d_{12}$ salts. Significant enhancement by deuteration of the charge-order phase transition temperature, $T_{CO}$, was observed in ESR measurements for all (TMTTF)$_2X$ salts measured. No obvious relation between the SbF$_6$ anion motion and the TMTTF charge-order was found by $^{19}$F NMR. We also performed single crystal X-ray measurements to understand the deuteration effects and temperature dependence of the crystal structure. A possible relationship between the $T_{CO}$'s and crystallographical parameters is proposed. The deuteration effects and possible origin of the charge-ordering transition of TMTTF salts are discussed.

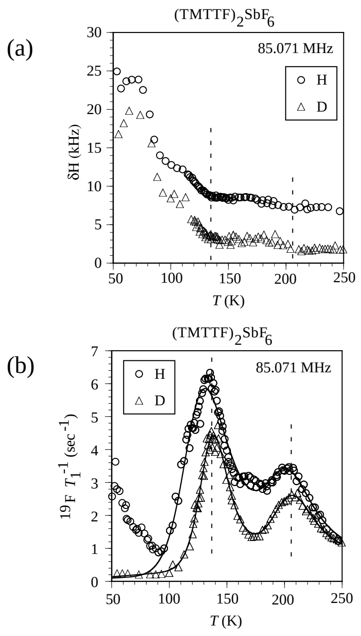

**Figure 1.** Temperature dependence of $^{19}$F NMR, (a) absorption full width at half maximum (FWHM) linewidth, δH, and (b) spin–lattice relaxation rate, $^{19}$F $T_1^{-1}$, of (TMTTF-$h_{12}$)$_2$SbF$_6$ (circle) and (TMTTF-$d_{12}$)$_2$SbF$_6$ (triangle). The solid lines are fitted results using the BPP equation.

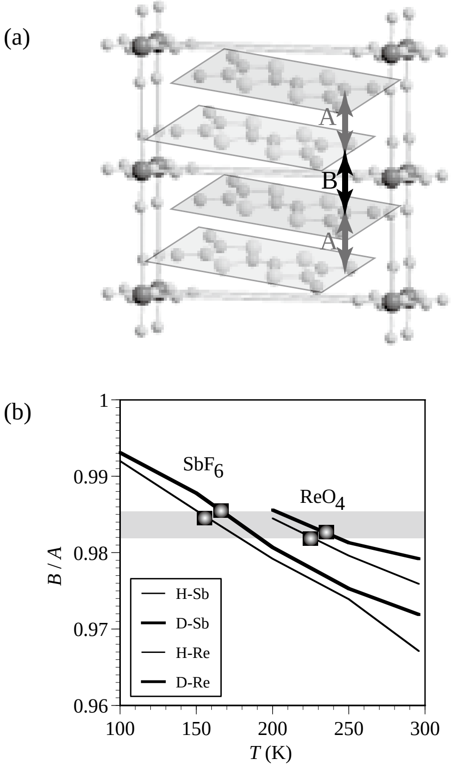

**Figure 2.** Crystal structure and definition of the inter-molecular distances, *A* and *B*, of (TMTTF)$_2$SbF$_6$. Temperature dependence of inter-molecular distances and their ratio of (TMTTF-$h_{12}$)$_2$SbF$_6$, (TMTTF-$d_{12}$)$_2$SbF$_6$, (TMTTF-$h_{12}$)$_2$ReO$_4$ and (TMTTF-$d_{12}$)$_2$ReO$_4$. The measured points (every 50 K) are interpolated with a straight line. Solid circles correspond to $T_{CO}$'s for each of salts.

## IV-B-2 $^{13}$C NMR Analyses of Successive Charge Ordering in (TMTTF)$_2$ReO$_4$

**NAKAMURA, Toshikazu; FURUKAWA, Ko; HARA, Toshifumi**

[*J. Phys. Soc. Jpn.* **75**, 013707 (4 pages) (2006)]

$^{13}$C NMR measurements were performed for a one-dimensional organic conductor, (TMTTF)$_2$ReO$_4$. The existence of an intermediate charge ordering (CO) phase was clarified for a TMTTF salt with a Td symmetry counter anion by the $^{13}$C NMR absorption line and spin-lattice relaxation rate, $^{13}$C $T_1^{-1}$. The $^{13}$C NMR spectra, which are characteristic of nuclei in equivalent molecules at room temperature, indicated two inequivalent molecules with unequal electron densities below 225 K. Moreover, the spin-singlet transition associated with ReO$_4$ anion ordering was confirmed at around 158 K by $^{13}$C NMR. The $^{13}$C NMR lines show a marked change at 158 K. The possible redistribution of the electronic charge at the anion ordering temperature as well as the origin of the charge ordering phenomena are discussed.

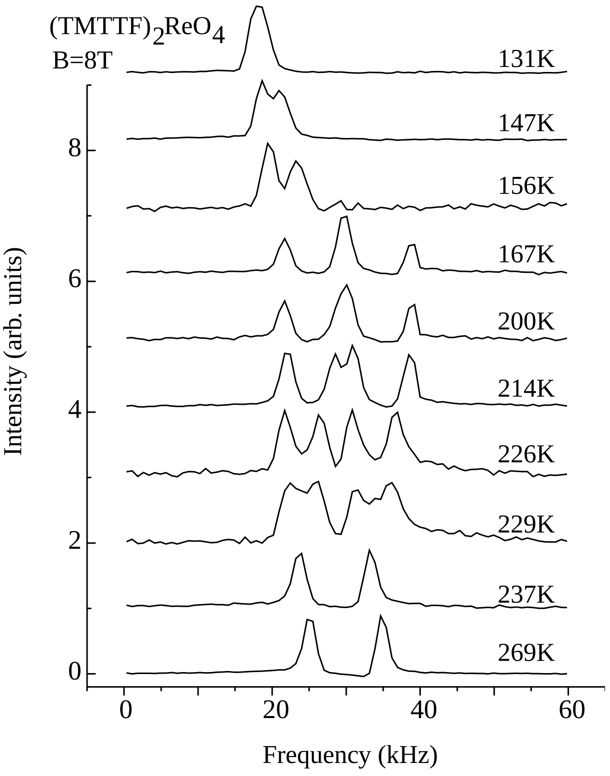

**Figure 1.** Temperature dependence of $^{13}$C NMR spectra of (TMTTF)$_2$ReO$_4$ Measurements were performed at the so-called magic-angle configuration.

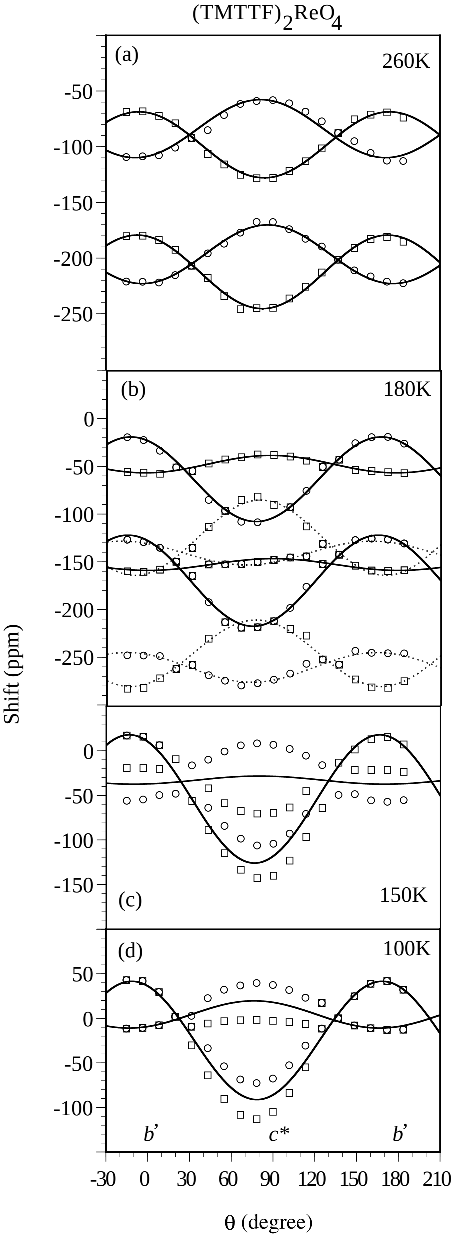

**Figure 2.** Angular dependence of resonance frequency of $^{13}$C NMR in (TMTTF)$_2$ReO$_4$. A single crystal of (TMTTF)$_2$ReO$_4$ was rotated within the *b'c** plane perpendicular to the external static magnetic field. The solid and dashed lines are included as guides to the eye, but are the least-squares fits to the measured data assuming the $3\cos^2\theta-1$ formulae.

## IV-B-3 Redistribution of Electronic Charges in the Spin-Peierls State in (TMTTF)$_2$AsF$_6$ Observed by $^{13}$C NMR

**FUJIYAMA, Shigeki; NAKAMURA, Toshikazu**

[*J. Phys. Soc. Jpn.* **75**, 014705 (7 pages) (2006)]

We report $^{13}$C NMR spectra and nuclear spin lattice relaxation rate $1/T_1$ for a quasi-one-dimensional quarter-filled organic material (TMTTF)$_2$AsF$_6$, which undergoes charge ordering ($T_{\rm CO}$ = 102 K) and spin-Peierls phase transitions ($T_{\rm SP}$ = 14 K). The ratio of two $1/T_1$ for the charge accepting and donating TMTTF sites which grows from $T_{CO}$ finally saturates in approaching $T_{SP}$, indicating one spin correlation function even in the charge ordered state. Below $T_{SP}$, however, the doubly split NMR lines from inequivalently charged molecules merge into one line, originated from the variation in charge densities. This shows that a rearrangement of the charge configuration occurs at $T_{SP}$.

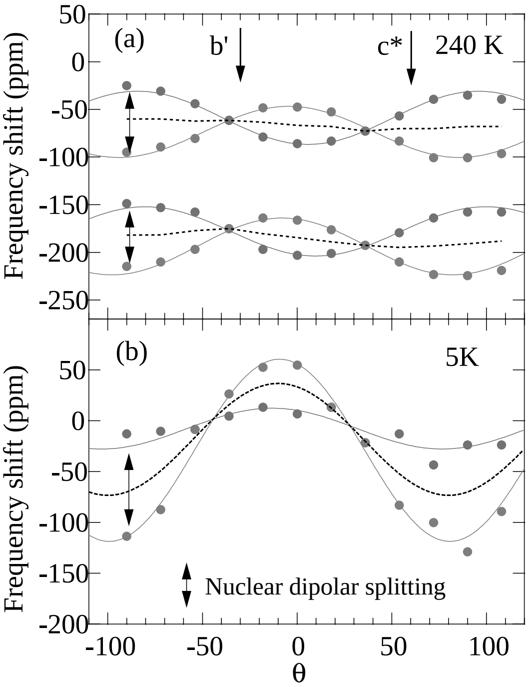

**Figure 1.** Angular dependence of the peak positions of the NMR spectra rotated in the *b–c* plane at 240 K (a) and 5 K (b).

## IV-B-4 The Effect of Deuteration on the Transition into a Charge Ordered State of $(TMTTF)_2X$ Salts

**NAD, Felix[1,2]; MONCEAU, Pierre[2]; NAKAMURA, Toshikazu; FURUKAWA, Ko**
*([1]Inst. Rad. Elec., Russia; [2]CNRS, France)*

[*J. Phys.: Condens. Matter* **17**, L399–L406 (2005)]

From dielectric permittivity measurements, we show that deuteration yields a large increase of the transition temperature for the charge ordered state of $(TMTTF)_2X$ ($X$ = $AsF_6$, $SbF_6$, $ReO_4$) salts. We propose an explanation of this phenomenon, suggesting that deuteration induces a modification of the $(TMTTF)_2X$ crystal unit cell.

## IV-B-5 Magnetic Properties of Hexa-*peri*-hexabenzocoronene Nanotube Investigated by Magnetic Resonance

**HARA, Toshifumi; FURUKAWA, Ko; NAKAMURA, Toshikazu; YAMAMOTO, Yohei[1]; KOSAKA, Atsuko[1]; FUKUSHIMA, Takanori[1,2]; AIDA, Takuzo[1,2]**
*([1]ERATO-SORST; [2]Univ. Tokyo)*

The discovery of electric conductive carbon nanotube materials has expanded interest in exploring novel materials for functional electronic devices. Recently, new type nanotubular objects has been developed by Aida and co-workers with novel HBC (hexa-*peri*-hexabenzocoronene) amphiphiles bearing hydrophilic oxyalkylene chains and lipophilic dodecyl chains. These HBC molecules stack to form a well-defined nanotube with a helical array of a large number of π-stacked HBC units. By chemical oxidation using iodine, the HBC nanotube turns to show highly electrical conductive behavior.

In order to understand the origin of the carrier and the electronic properties, ESR and $^1$H NMR measurements were carried out for the iodine doped HBC nanotube. The drastic increases of the ESR intensity with the iodine doping indicates that the carrier possesses a spin-freedom. In the initial phase of doping, a narrow ESR line was observed. After additional several hours of doping, another broad ESR lines appear, and the intensity of it overcomes that of the narrow lines. The spin susceptibility evaluated from the broad ESR line shows a temperature independent behavior down to 140 K. The ESR linewidth decreases with lowering temperature. These observations are typical phenomena of itinerant spins. Below 140 K, the spin susceptibility turns to show the Curie-like behavior, following an hump of ESR linewidth. The drastic change of the ESR parameters suggests a possible semiconductor to insulator transition (or crossover) in this nanotubular system. In this paper, we describe magnetic properties of the HBC nanotube and discuss the nature of the electronic phases from a microscopic point of view.

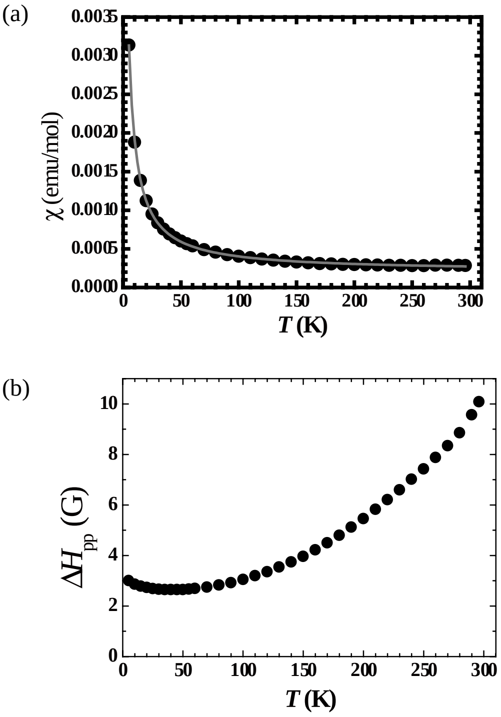

**Figure 1.** Temperature dependence of the spin susceptibility and ESR linewidth of the iodine doped HBC nanotube.

## IV-B-6 X-Ray Structural Study of Charge and Anion Orderings of TMTTF Salts

**NOGAMI, Yoshio[1]; ITO, Takayoshi[1]; YAMAMOTO,**

**Kenichiro[1]; IRIE, Naoaki[1]; HORITA, Shintaro[1]; KAMBE, Takashi[1]; NAGAO, Nobuaki[1]; OSHIMA, Kokichi[1]; IKEDA, Naoshi[2]; NAKAMURA, Toshikazu**
*([1]Okayama Univ.; [2]JASRI)*

[*J. Phys. IV France* **131**, 39–42 (2005)]

High resolution X-ray structure analyses and electronic structure calculation revealed the condition for the charge ordering (CO) observed in the $(TMTTF)_2X$ (Fabre) salts. The phase diagram of the electronic states including $2k_F$ and $4k_F$ CO has been proposed associated with magnitudes of molecular dimerization and tetramerization.

### IV-B-7 Depinning of the Spin-Density Wave in $(TMTTF)_2Br$ under Pressure

**NOMURA, Kazushige[1]; ISHIMURA, Kazunori[1]; FUJIMOTO, Kazuteru[1]; MATSUNAGA, Noriaki[1]; NAKAMURA, Toshikazu; TAKAHASHI, Toshihiro[2]; SAITO, Gunzi[3]**
*([1]Hokkaido Univ.; [2]Gakushuin Univ.; [3]Kyoto Univ.)*

[*J. Phys. IV France* **131**, 111–114 (2005)]

We have investigated the sliding motion of the SDW in the organic compound $(TMTTF)_2Br$ under the pressure with the measurement of the non-linear conductivity. Below the SDW transition temperature $T_{SDW}$, we observed the sharp increase of conductivity with the clear threshold electric field $E_T$, associated with the depinning of the SDW. For the typical sample, the temperature dependence of $E_T$ shows a peak around $0.3T_{SDW}$ in each pressure. In addition, the field hysteresis with the switching appears in the dc *I-V* characteristics around $0.3T_{SDW}$. The excess conductivity, dominated by the kinetic friction, shows a sharp increase below $0.3T_{SDW}$. These behaviors indicate that the sliding mechanism of SDW varies across $0.3T_{SDW}$, which is almost equal to the sub-phase transition temperature. This fact suggests that the transition at $0.37T_{SDW}$ is associated with both the magnetic and charge degrees of freedom.

### IV-B-8 Pulsed ESR Measurements for $(TMTTF)_2X$

**FURUKAWA, Ko; HARA, Toshifumi; NAKAMURA, Toshikazu**

It is well known that most of TMTTF salts undergo the charge ordering (CO) transitions in the paramagnetic phase. We already demonstrated the charge configuration pattern for several TMTTF salts. However it is not clear the relationship between the CO configurations and ground states. Actually, the $(TMTTF)_2SbF_6$ salts undergoes an antiferromagnetic phase, while the $(TMTTF)_2PF_6$ and $(TMTTF)_2AsF_6$ salts show spin-Peierls ground states. They have common CO configuration pattern at the paramagnetic phase. So it is interesting to investigate the charge configuration at around the spin-Peierls state. So we performed the pulsed ESR measurements for one of typical TMTTF salts, $(TMTTF)_2PF_6$ and $(TMTTF)_2Br$. The low temperature electron spin dynamics from the ESR point of view are discussed.

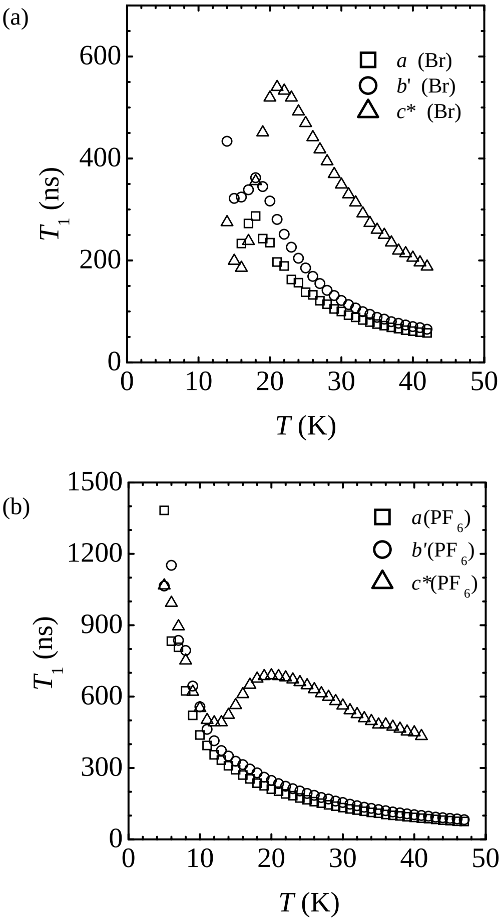

**Figure 1.** Temperature dependence of the ESR spin–lattice relaxation time, $T_1$, for $(TMTTF)_2Br$ (a) and $(TMTTF)_2PF_6$ (b).

### IV-B-9 Synchrotron X-Ray Diffraction Experiments and MEM Analyses for the Charge-Ordering State of $(TMTTF)_2PF_6$

**HARA, Toshifumi; FURUKAWA, Ko; NAKAMURA, Toshikazu; KAKIUCHI, Toru[1]; SAWA, Hiroshi[2]; IZUMI, Fujio[3]**
*([1]SOKENDAI; [2]KEK; [3]NIMS)*

TMTTF family salts have been attracting attention due to observations of their charge-ordering (CO) phenomena. $^{13}C$ NMR indicates the existence of inequivalent TMTTF sites at low temperatures, and dielectric permittivity measurements show ferroelectric behaviors for $(TMTTF)_2MF_6$ ($M$ = P, As, Sb) salts. We also proposed that the variation of charge-ordering patterns such as –O–O–o–o– and –O–o–O–o– along the stacking axes for a series of TMTTF salts by ESR linewidth analyses. The competition between the long-range Coulomb interaction and anion ordering are pointed out by experimental and theoretical investigations. However, there is no direct observation of the charge distribution for charge ordered states so far. Hence we performed synchrotron X-ray diffraction measurements and MEM analyses $(TMTTF)_2PF_6$ at R.T. and 20 K. We observed apparent difference of the electric charge distributions between two TMTTF molecules in the original unit cell. This fact reveals that the charge order phase transition in $(TMTTF)_2PF_6$ is purely electronic one without apparent structural changes.

### IV-B-10 *g*-Anisotropy of the $S_2$-State Manganese Cluster in Single Crystals of Cyanobacterial Photosystem II Studied by W-Band Electron Paramagnetic Resonance Spectroscopy

**MATSUOKA, Hideto[1]; FURUKAWA, Ko; KATO, Tatsuhisa[2]; MINO, Hiroyuki[3]; SHEN, Jian-Ren[4]; KAWAMORI, Asako[5]**
*([1]IMS and Free Univ. Berlin; [2]IMS and Josai Univ.; [3]Nagoya Univ.; [4]Okayama Univ.; [5]Kwansei Gakuin Univ. )*

[*J. Phys. Chem. B* **110**, 13242–13247 (2006)]

The multiline signal from the $S_2$-state manganese cluster in the oxygen evolving complex of photosystem II (PSII) was observed in single crystals of a thermophilic cyanobacterium *Thermosynechococcus vulcanus* for the first time by W-band (94 GHz) electron paramagnetic resonance (EPR). At W-band, spectra were characterized by the g-anisotropy, which enabled the precise determination of the tensor. Distinct hyperfine splittings (hfs's) as seen in frozen solutions of PSII at X-band (9.5 GHz) were detected in most of the crystal orientations relative to the magnetic field. In some orientations, however, the hfs's disappeared due to overlapping of a large number of EPR lines from eight crystallographic symmetry-related sites of the manganese cluster within the unit cell of the crystal. Analysis of the orientation-dependent spectral features yielded the following *g*-tensor components: $g_x = 1.988$, $g_y = 1.981$, $g_z = 1.965$. The principal values suggested an approximate axial symmetry around the Mn(III) ion in the cluster.

# IV-C Development of Multi-Functional Molecular Systems

Various types of molecular conductors such as organic superconducting alloys containing localized magnetic moments, single-component molecular metals with unprecedentedly high antiferromagnetic transition temperature, molecular conductors exhibiting resistivity anomaly coupled with a spin transition, and ferro- and ferri-electric porous molecular crystals were developed and their physical properties were examined. Recently, magnetic molecular conductors have attracted a considerable interest because of their possible *bi*-functional properties originated from the interaction between π conduction electrons and localized magnetic moments. But except BETS ( bis(ethyleneditio)tetrathiasfulvalene) conductors with $FeX_4^-$ (X = Cl, Br) anions developed more than ten years ago, there has been almost no organic superconductor (and even metal) exhibiting distinct *bi*-functional properties. In the last ten years, we have discovered unprecedented organic superconductors such as the system exhibiting "superconductor → insulator transition," the antiferromagnetic organic superconductors and the field-induced organic superconductors. We have recently re-examined the temperature-composition phase diagram of the alloys of organic superconductor (λ-$(BETS)_2GaCl_4$) and field-induced organic superconductor (λ-$(BETS)_2FeCl_4$) and found that the superconducting temperature phase of the alloy is stabilized by neighbouring on the antiferromagnetic insulating phase. In addition, we have reconfirmed the recently discovered peculiar "constant resistivity state" between zero-resistivity (or superconducting) state and normal metal state. It will be highly expected that new "vortex dynamics" will be disclosed in future from this unprecedented organic superconducting alloy.

Besides BETS conductors, we have developed new types of magnetic conductors such as (1) single-component molecular metal where conduction electrons and antiferromagnetic order coexists below 110 K, (2) novel system exhibiting weakly metallic behavior at high temperature and weak ferromagnetic properties at low temperature and (3) molecular conductors consisting of π molecule responsible for electron conduction and spin-crossover transition metal complex counter ion. We are also trying to synthesize new organic donors with stable radical spin parts and new functional porous molecular crystals.

We reported the improved method of four-probe resistivity measurements using diamond anvil several years ago. However we had to stop the high-pressure experiment since then. But we are now re-trying to perform the single-crystal resistivity measurements above 20 GPa.

## IV-C-1 Phase Diagram and Anomalous Resistivity Behavior of λ-$(BETS)_2Fe_xGa_{1-x}Cl_4$

**CUI, HengBo; TAKAHASHI, Kazuyuki; OKANO, Yoshinori; KOBAYASHI, Hayao; KOBAYASHI, Akiko[1]**
*([1]Nihon Univ.)*

Rich variety of organic conductors provides unique chances to encounter novel systems showing unexpected conducting phenomena such as s superconductor-to-insulator (SC-I) transition and organic thyristor effect. Several years ago, we have reported that λ-$(BETS)_2$ $FeCl_4$ undergoes a field-induced superconducting transition, where BETS (= bis(ethylenedithio)tetraselenafulvalene, $C_{10}H_8S_4Se_4$) is a π donor molecule. Since the size of $FeCl_4^-$ anion is almost equal to that of $GaCl_4^-$, unprecedented alloys (λ-$(BETS)_2Fe_xGa_{1-x}Cl_4$) of organic superconductor (λ-$(BETS)_2FeCl_4$) and field-induced organic superconductor) can be prepared at arbitrary mixing ratio. We have previously reported the temperature-composition (*T*-*x*) phase diagram of λ-$(BETS)_2Fe_x$ $Ga_{1-x}Cl_4$. However, we have recently found that *x*-value shows a significant difference even in one single crystal, which requested careful re-examination of the phase diagram of these novel alloy systems. The revised phase diagram showed that the superconducting phase is stabilized by neighboring on the antiferromagnetic insulating phase. In addition we have examined the resistivity behavior under magnetic field and found that constant resistivity state at $x = 0.37–0.42$.

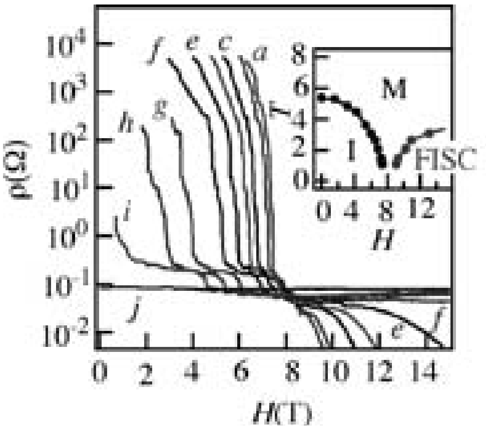

**Figure 1.** An example of *T*-*H* phase diagram of λ-$(BETS)_2Fe_x$ $Ga_{1-x}Cl_4$ ($x = 0.66$), where *H* is applied parallel to the *ac* conduction plane: $a = 1.1$ K, $b = 1.5$, $c = 2.1$, $d = 2.6$, $e = 3.1$, $f = 3.6$, $g = 4.45$, $h = 4.9$, $i = 5.3$, $j = 4.1$, $k = 7.7$. It is shown that the MI transition was suppressed around 8 T and the field-induced superconducting phase begins to appear.

## IV-C-2 Magnetic Transitions of Single-Component Molecular Metal $[Au(tmdt)_2]$ and Its Alloy Systems

**ZHOU, Biao[1]; KOBAYASHI, Akiko[1]; SHIMAMURA, Mina[1]; FUJIWARA, Emiko[1]; HIGASHI, Takeshi[2]; NISHIBORI, Eiji[2]; SAKATA, Makoto[2]; CUI, HengBo; TAKAHASHI, Kazuyuki; KOBAYASHI, Hayao**
*([1]Univ. Tokyo; [2]Nagoya Univ.)*

[*J. Am. Chem. Soc.* **128**, 3872–3873 (2006)]

$[Ni(tmdt)_2]$ (tmdt = trimethylenetetrathiafulvalenedithiolate) is the first single-component molecular metal, where the metal electrons can be automatically generated by self-assembly of single kind of molecules. Though $[Au(tmdt)_2]$ is isostructural to $[Ni(tmdt)_2]$, the electronic band structures is completely different from that of $[Ni(tmdt)_2]$ because the neutral bis(dithiolato)gold complex has an odd number of total electrons. Although it had been found that $[Au(tmdt)_2]$ undergoes a possible antiferromagnetic transition around 100 K, more detail examination was needed. We have recently succeeded to obtain high-quality sample and performed the single crystal structure determination, resistivity measurements (on compacted pellet sample) and magnetic susceptibility. As shown in Figure 1, the temperature and field dependences of the susceptibility showed antiferromagnetic transition at 110 K. Recent electrical resistivity measurements using interdegitated electrodes by Tanaka et al. confirmed that the crystal retains metallic state even below 100 K. Thus, $[Au(tmdt)_2]$ is clarified to be the first antiferromagnetic molecular metal with magnetic transition temperature at 110 K. The metallic state below the antiferromagnetic transition temperature is consistent with the band structure calculation suggesting the possibility of the partial nesting of the Fermi surfaces.

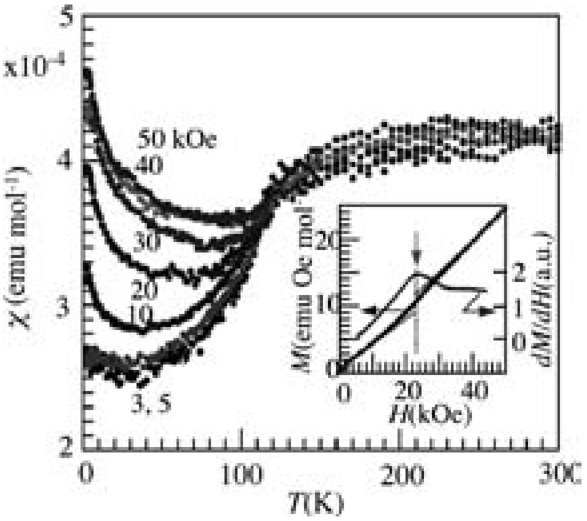

**Figure 1.** Temperature and magnetic field dependences of the susceptibilities of crystalline powder sample of $[Au(tmdt)_2]$. The inset is the *H*-dependences of *M* and *dM*/*dH* at 40 K. The gray arrow indicates the spin flop field

### IV-C-3 Molecular Design and Physical Properties of Single-Component Molecular Metals

**KOBAYASHI, Akiko**[1]**; OKANO, Yoshinori; KOBAYASHI, Hayao**
*([1]Univ. Tokyo)*

[*J. Phys. Soc. Jpn.* **75**, 051002 (2006)]

The design of metallic crystals consisting of single-component molecules (*single-component molecular metal*) is explained on the basis of the examinations of frontier molecular orbitals and the simple extended-Hückel tight-binding band pictures. To meet the conditions required to realize automatic carrier generation by self-assembly of the same kind of neutral molecules, a crystal of a transition metal complex molecule $[Ni(tmdt)_2]$ with extended-TTF-type (TTF = tetrathiafulvalene) dithiolate ligands was synthesized, which was found to be the first single-component molecular metal. The X-ray structure analyses of the crystals of $[(C_4H_9)_4N]_2[Ni(tmdt)_2]$ and neutral $[Ni(tmdt)_2]$ provided information on the symmetry of the frontier molecular orbitals (the highest occupied molecular orbital (HOMO) and the lowest unoccupied molecular orbital (LUMO)) from which the metallic bands are formed. The infrared and visible spectra of a crystalline powder sample of $[Ni(tmdt)_2]$ showed a broad electronic absorption maximum at around 2200 $cm^{-1}$, suggesting an extremely small HOMO-LUMO gap. The physical properties of some of the hitherto-developed single-component molecular conductors are also briefly described.

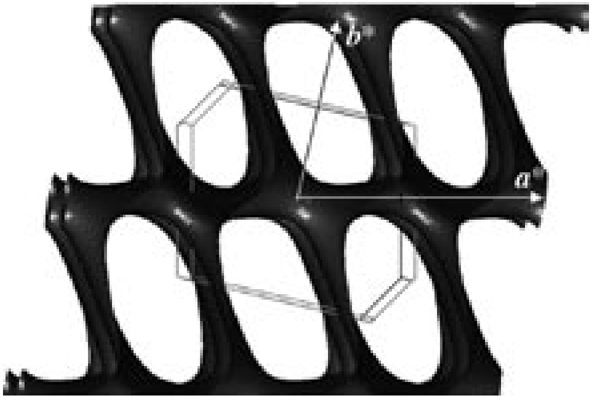

**Figure 1.** Fermi surfaces of single-component magnetic molecular metal, $[Au(tmdt)_2]$ viewed along the $c^*$ direction.

### IV-C-4 A Molecular Conductor Based on Monoanionic Nickel Complex with Extended-TTF Type Ligands, $(^nBu_4N)[Ni(dmstfdt)_2]$ Exhibiting Weakly Metallic Behavior at High Temperature and Weak Ferromagnetism at Low Temperature

**FUJIWARA, Emiko**[1]**; YAMAMOTO, Kimiko**[1]**; SHIMAMURA, Mina**[1]**; ZHOU, Biao**[1,2]**; KOBAYASHI, Akiko**[1,2]**; CUI, HengBo; TAKAHASHI, Kazuyuki; OKANO, Yoshinori; KOBAYASHI, Hayao**
*([1]Univ. Toky; [2]Nihon Univ.)*

A 1:1 tetrabutylammonium nickel complex with TTF-type ligands, $(^nBu_4N)[Ni(dmstfdt)_2]$ (dmstfdt = dimethyldiselenadithiafulvalenedithiolate) (**1**) is a unique molecular system with ambivalent character which exhibits weakly metallic behavior above room temperature and a weak ferromagnetism of localized electrons at low temperature. The X-ray structure analysis of **1** revealed that there are crystallographically independent two $[Ni(dmstfdt)_2]^-$ anions (A and B) and two $^nBu_4N^+$ cations in the unit cell. The anions are arranged in a zigzag –ABA'B'– manner along the molecular side-by-side direction with a dihedral angle of molecular planes being 42.6°. The tight-binding band structure calculation based on the extended Hückel approximation of **1** gave small three-dimensional electron and hole Fermi surfaces, which were compatible with the observed weakly metallic behavior around room temperature despite of the 1:1 stoichiometry of the complex. The $\chi T$ values of **1** increased linearly from 0.129 to 0.383 emu·K·mol$^{-1}$ with decreasing temperature at 160–340 K, suggesting the gradual electron localization with lowering temperature. At 147 K, the complex **1** showed a sharp insulating transition associated with the localization of one electron on each nickel complex below 160 K. At 80–150 K, $\chi$ was well fitted by the Curie-Weiss law: $\chi = C/(T–\theta)$; $C$ = 0.383 emu·K·mol$^{-1}$ and $\theta$ = –4 K. A weak ferromagnetism was observed below 7 K. The coercive force was ±1.5 kOe at 2.0 K.

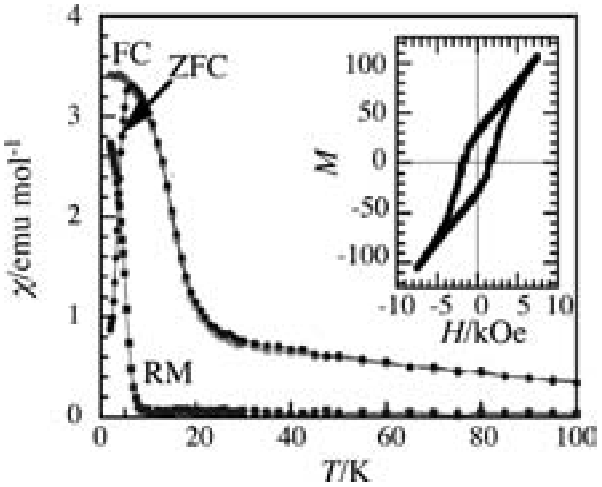

**Figure 1.** The zero-field-cooled (ZFC) and field-cooled (FC) susceptibilities and remnant magnetization (RM) as a function of temperature at 1 kOe for the polycrystalline sample of **1**. The insets shows the field dependence of the magnetization at 2.0 K.

## IV-C-5 Ferroelectric Porous Molecular Crystal, $[Mn_3(HCOO)_6](C_2H_5OH)$

**CUI, HengBo; WANG, Zheming[1]; TAKAHASHI, Kazuyuki; OKANO, Yoshinori; KOBAYASHI, Hayao; KOBAYASHI, Akiko[2]**
*([1]Peiking Univ.; [2]Nihon Univ.)*

Weak interaction is the most characteristic feature in the assembling of molecules. A typical example is the host-guest interaction in the porous materials, which have recently attracted large attention because of the high potentiality in the design of new materials with novel functions. Since the polar guest molecules form small assemblies loosely confined in the porous space, the porous material will be easily converted to the highly polarizable system by inserting polar guest molecules. If the polarized guest molecules are three-dimensionally ordered, a ferro- (or antiferro-) electric state will be realized. Furthermore, if we can combine the ferroelectrically polarizable guest molecules and the host porous lattice exhibiting magnetic order, we can obtain new type of "*multiferroic* molecular materials" where ferroelectricity and ferromagnetism coexist. We have recently discovered the first example of porous molecular crystal $[Mn_3(HCOO)_6](C_2H_5OH)$ exhibiting ferroelectric transition at 165 K and ferrimagnetic transition at 8.5 K. The temperature dependence of the dielectric constants indicated that the ferroelectric transition is the first order transition. The dielectric measurements on the crystal with deuterated ethanol showed no significant change of $T_c$, suggesting that H-bond is not play an important role.

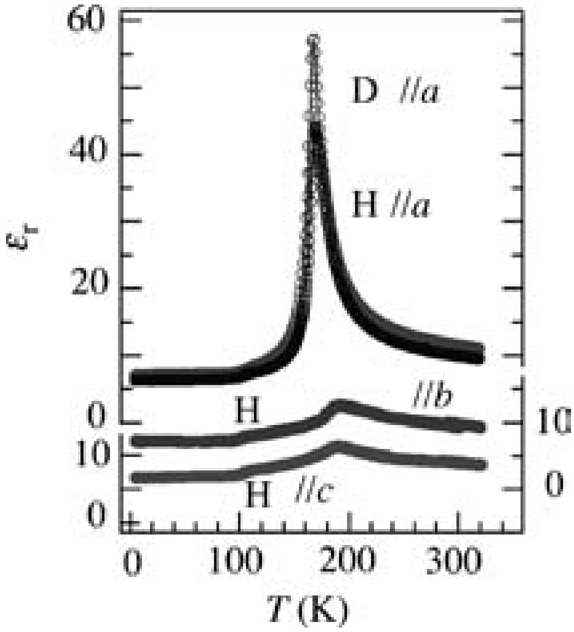

**Figure 1.** Dielectric constants ($\varepsilon_r$) of $[Mn(HCOO)_6](C_2H_5OH)$ for the field *E*//*a*, *b* and *c*. The $\varepsilon_r$ (*E*//*a*) of the crystal with deuterated ethanol, $[Mn(HCOO)_6](C_2H_5OD)$ is also presented (open circles). D and H represent the dielectric constants of $[Mn(HCOO)_6](C_2H_5OH)$ and $[Mn(HCOO)_6](C_2H_5OD)$, respectively.

## IV-C-6 Antiferroelect Porous Molecular Crystal with Guest Water Molecules

**CUI, HengBo; LONG, La-Sheng[1]; TAKAHASHI, Kazuyuki; OKANO, Yoshinori; KOBAYASHI, Hayao; KOBAYASHI, Akiko[1]**
*([1]Xiamen Univ.; [2]Nihon Univ.)*

We have recently found that a porous molecular crystal containing guest $H_2O$ molecules, $[Cu_3La_2$(imino diacetate)$_3](H_2O)_8$ exhibits anomalously large dielectric constants and antiferroelectric hysteresis above the room temperature. At first, we measured the dielectric constants of the crystalline powder sample. But it gave anomalously large dielectric constant. In addition, the dielectric constant increased with increasing temperature around the room temperature. Similar behaviors were observed in various powdered crystals including famous ferroelectric material such as $KH_2PO_4$, which of course gave normal results when the single crystal was used. Therefore the measurement using the single crystal is essential for the dielectric experiments. In the present studies, the crystal with the size of 1.4 × 1.1 × 0.55 mm$^3$ was used. As shown in Figure 1, $\varepsilon_r$ showed a characteristic temperature dependence above 150 K. Though $\varepsilon_r$ of $[Cu_3La_2$(iminodiacetate)$_6](H_2O)_8$ increased above 250

K, its temperature dependence became sluggish above 340 K. It was quite surprising that the antiferroelectric hysteresis loop was observed around 350 K where the guest $H_2O$ molecules began to escape fairly rapidly. The dielectric properties of $[Cu_3La_2(iminodiacetate)_6](D_2O)_8$ were also examined.

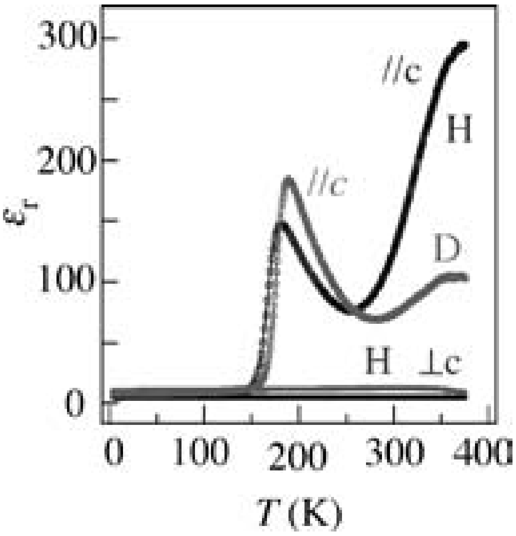

**Figure 1.** The dielectric constants $\varepsilon_r$ of $[Cu_3La_2(iminodiacetate)_6](H_2O)_8$ for *E*//*c* (black) and *E*⊥*c* (gray). The black lines indicate $\varepsilon_r$ of the guest-free crystal $[Cu_3La_2(iminodiacetate)_6]$. The dielectric constant of $[Cu_3La_2(iminodiacetate)_6](D_2O)_8$ is also presented (*E*//*c* (gray)).

## IV-C-7 High-Pressure Four-Probe Resistivity Measurements of Organic Crystals

**CUI, HengBo; KOBAYASHI, Hayao**

It is well known that resistivity measurements at extremely high pressure using diamond anvil revealed the superconductivities of various molecular materials such as hexa-iodobenzene and even $O_2$ which are usually considered to have no connection with electron conduction phenomena. Although the diamond anvil technique is very attractive one, its application to the four-probe resistivity measurements of the fragile organic crystals seems to contain many difficulties. Non-hydrostatic nature of the pressure medium at high pressure and anisotropic nature of molecular crystals will prevent the accurate resistivity measurements. However, the largest difficulty will exists in the method to connect four electrical leads (usually very thin gold wires) bonded to small sample crystal set in the small sample space in the diamond anvil cell with four lead terminals outside the diamond anvil. Several years ago, we have reported the superconductivity of $(TMTTF)_2PF_6$ discovered around 5 GPa by four-prove diamond anvil resistivity measurements and the improved method of the diamond anvil resistivity measurements. Very recently we have re-tried to perform high-pressure resistivity measurements of organic crystals by adopting the same method and found this method to be applicable at least up to 20 GPa.

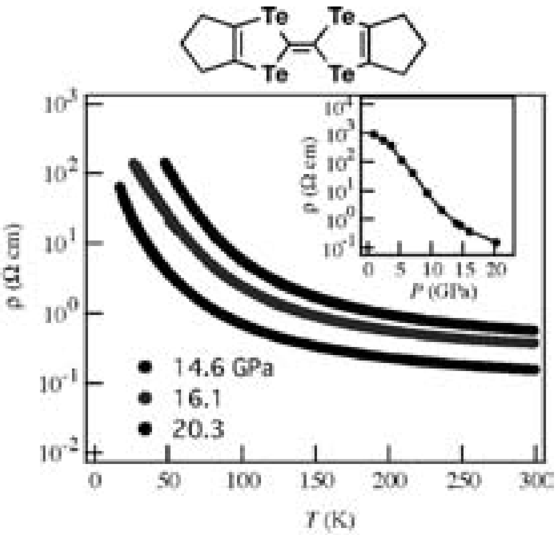

**Figure 1.** An example of the temperature dependence of the resistivity of molecular crystal up to 20 GPa. It should be noted that the room-temperature resistivity of the crystal of HMTTeF was reduced to about 0.15 Ωcm at 20 GPa.

## IV-C-8 Electrical Conductivity Modulation Coupled to a High-Spin–Low-Spin Conversion in the Molecular System $[Fe^{III}(qsal)_2][Ni(dmit)_2]_3 \cdot CH_3CN \cdot H_2O$

**TAKAHASHI, Kazuyuki; CUI, HengBo; OKANO, Yoshinori; KOBAYASHI, Hayao; EINAGA, Yasuaki[1]; SATO, Osamu[2]**
*([1]Keio Univ.; [2]Kyushu Univ.)*

[*Inorg. Chem.* **45**, 5739–5741 (2006)]

Recently considerable interest has been attracted to the development of novel multi-functional molecular conductors. We have attempted to explore the possibility of reversible control of electrical conducting states by external stimuli. It is well known that the conducting properties of molecular conductors are changed greatly by the small modification of their crystal structures. Since the spin transition between the low-spin (LS) and the high-spin (HS) states accompanies a remarkable structural change in coordination bond length and geometry, the electrical conductivity of conducting spin-crossover (SCO) complex can be expected to be controlled by a structural change involving the spin conversion. The title complex was prepared by applying a constant voltage of $[Fe(qsal)_2][Ni(dmit)_2] \cdot 2CH_3CN$ in acetonitrile [qsalH = *N*-(8-quinolyl)-salicylaldimine, dmit = 4,5-dithiolato-1,3-dithiole-2-thione]. $Ni(dmit)_2$ molecules are arranged in a face-to-face manner to form a six-fold column along the *b* axis. These columns are arranged in a herring-bone type side-by-side to generate layers along the transverse direction. $Fe(qsal)_2$ cations are dimerized by π–π interactions. The $Fe(qsal)_2$ dimers construct a one-dimensional chain parallel to the Fe–Fe direction of a dimer, which is the *a*+*b* direction in the present case. Thus, $Fe(qsal)_2$ chains were interwoven with the $Ni(dmit)_2$ columns. Temperature dependence of magnetic moment and electrical resistivity of the 1:3 complex were shown in Figure 1. Interestingly, a hysteresis loop of resistivity was observed in the temperature range of 90–120 K, which corresponds to the temperature range of the hysteresis of magnetic behavior. The relatively low resistivity in the heating process may be due to a sort of “chemical pressure effect” associated with the spin transition. Since the smaller size of SCO ions in the LS state than in the HS state will produce the more compact molecular packing of the cationic layers; this contraction exerts a pressure to the Ni(dmit)$_2$ conducting layers to make the system more conducting. Thus, to the best of our knowledge, this is the first evidence of a resistivity anomaly coupled with a spin transition in the SCO-molecular conductor hybrid.

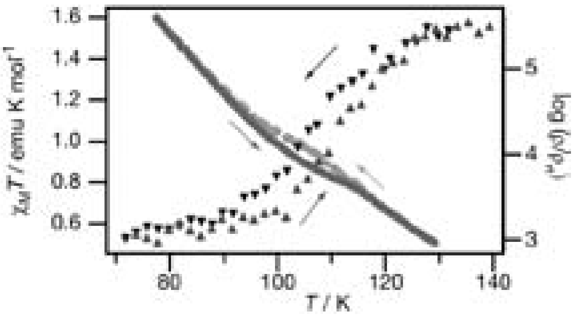

**Figure 1.** $\chi_M T$ *vs.* $T$ plot (triangle, scale: left) and log($\rho/\rho_{rt}$) *vs.* $T$ plot (circle, scale: right) of the 1:3 complex at the temperature range between 70 and 140 K.

### IV-C-9 Structural Modifications Accompanying a Reproducible Spin-Crossover Phenomenon in [Fe(qsal)$_2$][Ni(dmise)$_2$]·2CH$_3$CN

**TAKAHASHI, Kazuyuki; CUI, HengBo; KOBAYASHI, Hayao; EINAGA, Yasuaki[1]; SATO, Osamu[2]**
*([1]Keio Univ.; [2]Kyushu Univ.)*

Recently we have developed novel Fe(III) spin-crossover (SCO) systems containing the Ni(dmit)$_2$ components: [Fe(qsal)$_2$][Ni(dmit)$_2$]·2CH$_3$CN showed a cooperative spin transition and a light-induced excited spin state trapping (LIESST) effect and [Fe(qsal)$_2$][Ni(dmit)$_2$]$_3$·CH$_3$CN·H$_2$O demonstrated a conducting modulation coupled to a spin transition [qsalH = *N*-(8-quinolyl)-salicylaldimine, dmit = 4,5-dithiolato-1,3-dithiole-2-thione]. In particular, the synergic behavior between conducting and magnetic properties probably results from a sort of “chemical pressure effect” involving a spin conversion. However, it has never been successful to determine the crystal structures before and after the spin transition in both complexes. In the course of further studies to investigate more conducting systems in the related complexes, a reproducible spin transition with a small hysteresis loop that didn’t change by repeating the cooling and heating treatments was found in [Fe(qsal)$_2$][Ni(dmise)$_2$]·2CH$_3$CN [dmise is 4,5-dithiolato-1,3-dithiole-2-selone] (Figure 1). The crystal structure in the high temperature (HT) phase was isostructural to that of [Fe(qsal)$_2$][Ni(dmit)$_2$]·2CH$_3$CN at room temperature. The crystal system and symmetry does not change in the low temperature (LT) phase. Fe(qsal)$_2$ molecules formed one-dimensional chains through strong π–π interactions along the *b* axis and each chain was overlapped each other, to construct Fe(III) cation two-dimensional layers. The coordination bond lengths around the Fe atom indicated that the Fe(III) complex in the HT phase was almost in the high spin state and that in the LT phase was almost in the low spin state, respectively. These observations are consistent with the $\chi_M T$ values calculated from the SQUID data. A significant contraction in Fe(qsal)$_2$ two-dimensional layer was observed from the HT to the LT phases, suggesting this contraction would apply pressure to Ni(dmit)$_2$ layers.

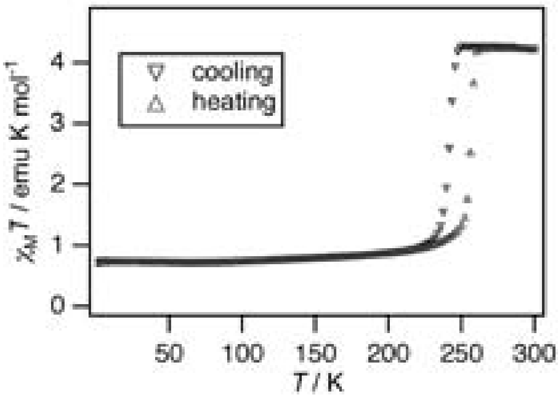

**Figure 1.** $\chi_M T$ *vs.* $T$ plot of [Fe(qsal)$_2$][Ni(dmise)$_2$]·2CH$_3$CN.

### IV-C-10 A Magnetic Organic Conductor Based on a π Donor with a Stable Radical and a Magnetic Anion—A Step to Magnetic Organic Metals with Two Kinds of Localized Spin Systems

**OTSUBO, Saika; CUI, HengBo; LEE, HaJin; FUJIWARA, Hideki; TAKAHASHI, Kazuyuki; OKANO, Yoshinori; KOBAYASHI, Hayao**

[*Chem. Lett.* **35**, 130–131 (2006)]

The synergetic action of magnetism and conductivity in the magnetic organic conductor consisting of π donor molecules and magnetic anions has recently attracted a considerable attention. On the other hand, there remains the long-standing target, that is, the magnetic organic conductor based on π donors having a stable organic radical part in the development of magnetic organic conductors. We have utilized a stable radical donor, TTP-PROXYL, which is 2,5-bis(1,3-dithiol-2-ylidene)-1,3,4,6-tetrathiapentalene (TTP) incorporating the 2,2,5,5-tetramethyl-1-pyrrolidin-1-yloxyl (PROXYL) radical, and have obtained two isostructural conducting salts, (TTP-PROXYL)FeCl$_4$ and (TTP-PROXYL)GaCl$_4$. (TTP-PROXYL)FeCl$_4$ is a semiconductor with two kinds of localized spin systems which are organic radical spins and 3d spins of magnetic FeCl$_4^-$ ions, respectively. Compared with the isostructural GaCl$_4$ salt showing similar conducting properties, the π spin of the TTP-PROXYL radical cation disappears due to dimerization but the $\chi T$-value in FeCl$_4$ salt is 4.65 K emu mol$^{-1}$, indicating the coexistence of high-spin Fe$^{3+}$ ($S$ = 5/2) and PROXYL radical ($S$ = 1/2). This observation will open a way to realize a new type of the magnetic organic conductors such as ferrimagnetic organic conductors.

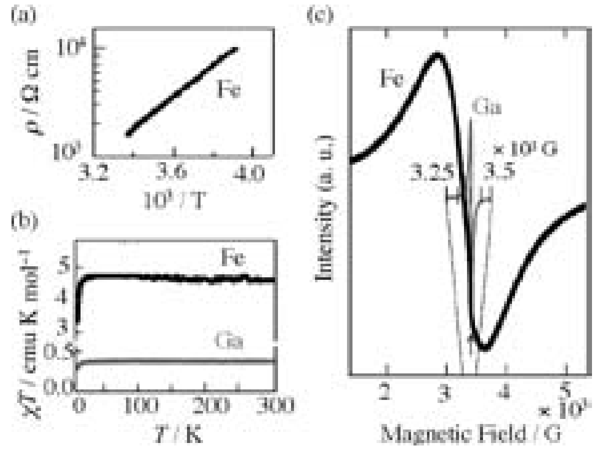

**Figure 1.** (a) Temperature dependence of the resistivity of (TTP-PROXYL)$FeCl_4$. (b) The $\chi T$-$T$ plots of (TTP-PROXYL)$MCl_4$ (M = Fe, Ga). (c) ESR spectra of (TTP-PROXYL)$MCl_4$ at 3.5 K.

## IV-C-11 Synthesis and Characterization of Novel PROXYL-Fused π-Electron Donors

**TAKAHASHI, Kazuyuki; KOBAYASHI, Hayao**

The development of novel magnetic molecular conductors based on the interplay between conducting electrons and localized spins has aroused a great attention in molecular materials science. To realize the coupling between conducting π-electrons and the spins on the stable organic radical in purely organic systems is one of the targets in this field. Despite several reports of syntheses and physical properties of π-electron donor or acceptor molecules with stable organic radicals and their conducting complexes, the number of well-characterized conducting complexes based on these donor or acceptor molecules is rare. Probably since the organic stable radicals are usually bulky and flexible, it is difficult to construct the conduction path based on the overlap between π-donors or acceptors and to give conducting crystals of good quality. In order to decrease a steric hindrance of a stable organic radical and to make a molecular structure rigid, we have designed and synthesized novel PROXYL radical-fused diselenadithiafulvalene (STF) derivatives. All the spectral data of new radical donors were in a good agreement with their molecular structures. Cyclic voltammograms revealed that the first and second one-electron oxidations occurred on the STF moieties, suggesting the possibility to generate cation biradical species. PROXYL-ET-STF afforded the 1:1 charge transfer complex with $TCNQF_4$. The radical donors (D) and acceptors (A) were alternately stacked to form irregular one-dimensional columns consisted of D–A–D trimers and A monomers (Figure 1). Bond length differences indicated that the complete charge transfer from the donor to the acceptor would occur. The magnetic data suggested that π-spins on the donor and acceptor were strongly antiferromagnetically coupled. The existence of NO radical spins was also suggested.

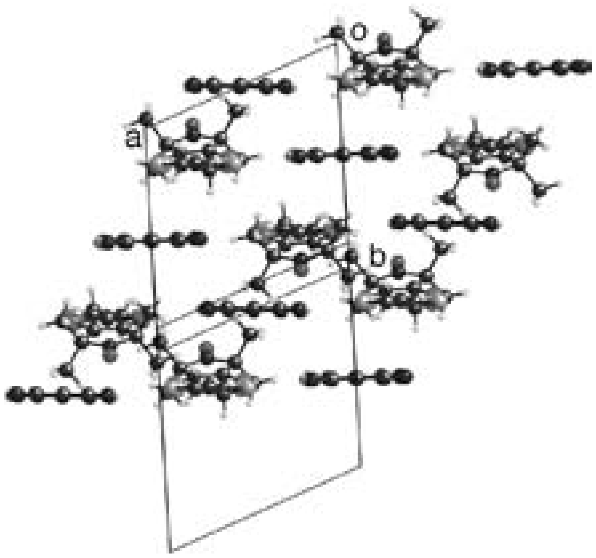

**Figure 1.** Crystal structure of (PROXYL-ET-STF)($TCNQF_4$)·PhCl.

# IV-D Progress of Conjugated Phenomena Coupled with Spin, Charge and Photon for Assembled Hetero-Molecular System

Intercalation of photochromic molecule into magnetic system provides fascinating multi-functionalities such as photo-magnetism, which gains much attention for their application to devices. The main subjects in this project are the development of photo-induced spin-crossover phenomena at room temperature by using the photo-isomerization of intercalated molecule, and the development of the transformation of magnetism for two-dimensional ferromagnetic system coupled with photochromic molecule.

## IV-D-1 Enhancement of the Curie Temperature by Photoisomerization of Diaryl-Ethene (DAE) for an Organic–Inorganic Hybrid System: $Co_4(OH)_7(DAE)_{0.5}{\cdot}3H_2O$

**SHIMIZU, Hideharu**[1]**; NAKAMOTO, Akio**[1]**; ENOMOTO, Masaya**[1]**; KOJIMA, Norimichi**[2]
*([1]Univ. Tokyo; [2]IMS and Univ. Tokyo)*

[*Inorg. Chem.* **45**, 10240–10247 (2006)]

Photomagnetism is one of the most attractive topics in recent research on molecular solids. Intercalation of an organic photochromic molecule into layered magnetic systems has a possibility to provide multifunctional properties such as photomagnetism. In order to build up a photosensitive multifunctional magnet, an organic-inorganic hybrid system coupled with a photochromic diarylethene anion, 2,2’-dimethyl-3,3’-(perfluorocyclopentene-1,2-diyl)bis(benzo[b]thiophene-6-sulfonate) (DAE), and cobalt LDHs (layered double hydroxides), $Co_4(OH)_7(DAE)_{0.5}{\cdot}3H_2O$, was synthesized by the anion exchange reaction between $Co_2(OH)_3(CH_3COO){\cdot}H_2O$ and DAE.[1,2] In the dark and under UV (313 nm) irradiated conditions, $Co_4(OH)_7(DAE)_{0.5}{\cdot}3H_2O$ with the open and close-forms of DAE were obtained, respectively. The magnetic susceptibility measurements elucidated ferromagnetic intra- and inter-layer interactions and Curie temperatures of $T_C = 9$ K and $T_C = 20$ K for cobalt LDHs with the open and close-forms of DAE, respectively. The enhancement of the Curie temperature from 9 K to 20 K by substituting the open-form of DAE with the close-form of DAE as intercalated molecule is attributed to the delocalization of π electrons in the close-form of DAE, which enhances the inter-layer magnetic interaction. The enhancement of the inter-layer magnetic interaction induced by the delocalization of π electrons in intercalated molecules is strongly supported by the fact that the Curie temperature (26.0 K) of cobalt LDHs with (*E*,*E*)-2,4-hexadienedioate having a conjugated π electron system is enormously higher than that (7.0 K) of cobalt LDHs with hexanedioate, which is shown in Figure 1.[2] By UV irradiation of 313 nm, $Co_4(OH)_7(DAE)_{0.5}{\cdot}3H_2O$ shows the photoisomerization of DAE from the open-form to the close-one in solid state, which leads to the enhancement of Curie temperature, which is schematically shown in Figure 2.[2]

**References**
1) M. Okubo, M. Enomoto and N. Kojima, *Solid State Commun.* **134**, 777 (2005).
2) H. Shimizu, M. Okubo, A. Nakamoto, M. Enomoto and N. Kojima, *Inorg. Chem.* **45**, 10240 (2006).

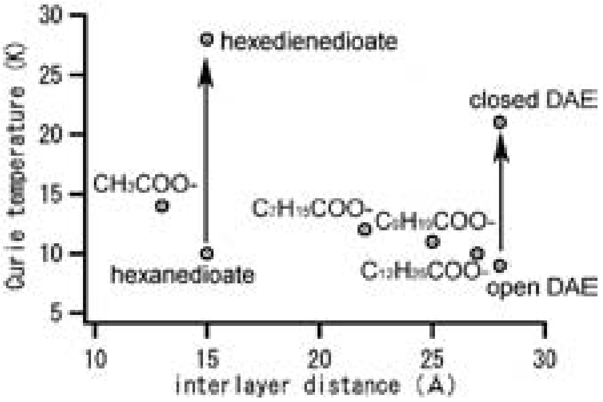

**Figure 1.** Relation between the interlayer distance and the Curie temperature of Co-LDHs.

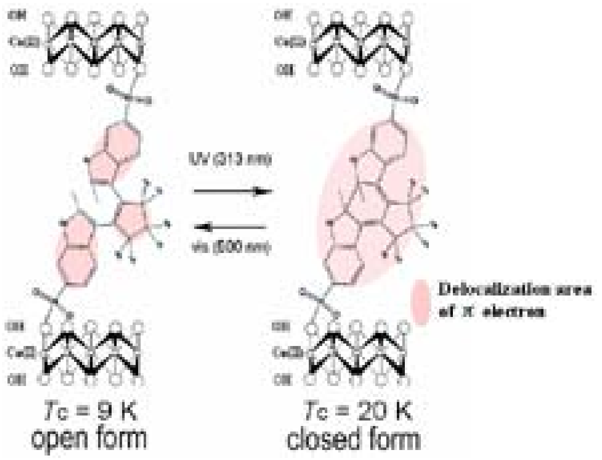

**Figure 2.** Schematic representation of the photoinduced conversion between Co-LDHs with open-form of DAE having $T_C = 9$ K and Co-LDHs with closed-form of DAE having $T_C = 20$ K.

## IV-D-2 Charge Transfer Phase Transition and Ferromagnetism in Organic- Inorganic Hybrid System, $A[Fe^{II}Fe^{III}(dto)_3]$($A = (C_nH_{2n+1})_4N$, Spiropyran, *etc.*; dto = $C_2O_2S_2$)

**KOJIMA, Norimichi**[1]**; HIKITA, Masanori**[2]**; KIDA, Noriyuki**[2]**; KASHIMA, Izuru**[2]**; ONO, Yuuki**[2]**; ITOI, Miho**[2]**; ENOMOTO, Masaya**[2]
*([1]IMS and Univ. Tokyo; [2]Univ. Tokyo)*

[*Synth. Met.* **153**, 473–476 (2005), *Eur. J. Inorg. Chem.* 1198–1207 (2006)]

In the case of mixed-valence complexes whose spin states are situated in the spin-crossover region, it is expected that new types of conjugated phenomena coupled with spin and charge take place. Recently, we have discovered a new type of first order phase transition around 120 K for $(n\text{-}C_3H_7)_4N[Fe^{II}Fe^{III}(dto)_3]$(dto = $C_2O_2S_2$), where the thermally induced charge transfer between $Fe^{II}$ and $Fe^{III}$ occurs reversibly.1) $(n\text{-}C_4H_9)_4N[Fe^{II}Fe^{III}(dto)_3]$ also undergoes the charge transfer phase transition around 140 K, while the charge transfer phase transition does not take place for $(n\text{-}C_nH_{2n+1})_4N[Fe^{II}Fe^{III}(dto)_3]$($n$ = 5 and 6), where the spin configuration of $Fe^{II}$ ($S$ = 2) and $Fe^{III}$ ($S$ = 1/2) exists between 2 K and 300 K. Moreover, $(n\text{-}C_nH_{2n+1})_4N[Fe^{II}Fe^{III}(dto)_3]$ ($n$ = 3–6) undergo the ferromagnetic phase transition. The Curie temperatures for $n$ = 3 and 4 are 6.5 K and 6 K & 13 K, respectively, while those for $n$ = 5 and 6 are 19 K and 25 K, respectively.2)

As mentioned above, these phase transitions remarkably depend on the size of intercalated cation, which implies a possibility to control the magnetic properties of two-dimensional honeycomb network structure of $[Fe^{II}Fe^{III}(dto)_3]_\infty$ by means of the isomerization of intercalated cation. From this viewpoint, we have synthesized a photo-sensitive organic-inorganic hybrid system, $(SP)[Fe^{II}Fe^{III}(dto)_3]$(SP = spiropyran), and investigated the photo-induced effect on the magnetic properties through the medium of photo-isomerization of spiropyran.3) When the UV light is irradiated for $(SP)[Fe^{II}Fe^{III}(dto)_3]$ in KBr pellet between 300 K and 77 K, a new absorption spectrum with wide half-width appears around 550 nm, which corresponds to the $\pi$-$\pi^*$ transition in the open form of $SP^+$, which implies that the photo-isomerization of $SP^+$ takes place even at 77 K in the solid state of $(SP)[Fe^{II}Fe^{III}(dto)_3]$. The zero-field cooled magnetization (ZFCM) has two peaks at 5 K and 15 K, which implies the coexistence of two ferromagnetic phases. The peak of ZFCM at 5 K disappears after UV irradiation. These UV irradiation effects on the magnetic properties imply that the photo-isomerization of SP from the closed form to the open one stabilizes the high-temperature phase with $Fe^{III}$($S$ = 1/2)–$Fe^{II}$($S$ = 2) and destabilizes the low-temperature phase with $Fe^{III}$($S$ = 5/2)–$Fe^{II}$($S$ = 0). Consequently, it is concluded that the charge transfer transition between $Fe^{II}$ and $Fe^{III}$ in $[Fe^{II}Fe^{III}(dto)_3]$ is induced by the photo-isomerization of SP in $(SP)[Fe^{II}Fe^{III}(dto)_3]$.

**References**

1) N. Kojima, W. Aoki, M. Itoi, Y. Ono, M. Seto, Y. Kobayashi and Yu. Maeda, *Solid State Commun.* **120**, 165 (2001).

2) M. Itoi, Y. Ono, N. Kojima, K. Kato, K. Osaka and M. Takata, *Eur. J. Inorg. Chem.* 1198 (2006).

3) I. Kashima, M. Okubo, Y. Ono, M. Itoi, N. Kida, M. Hikita, M. Enomoto and N. Kojima, *Synth. Met.* **153**, 473 (2005).

# IV-E Charge and Spin Dynamics of Organic Conductors

The spin and charge dynamics in organic conductors play important role in the emergence of the exotic properties in organic conductors, for example, superconductivity, magnetic ordering, charge ordering. For these purposes, it is important to reveal not only magnetic properties, the total picture of organic conductors. As known well, $^{13}$C-NMR is a one of the most powerful tool in the point of the magnetism. Since nuclear magnetic moment, $I$, is 1/2, $^{13}$C-NMR is not sensitive to the charge properties. On the other hand, optical studies, which are sensitive to the charge properties, are complementary to NMR study. In order to study both magnetic and charge properties, we performed $^{13}$C-NMR and optical works.

## IV-E-1 Charge Ordering State on Organic Conductors

**OGURA, T.[1]; KAWAMOTO, Atsushi[2]; KUMAGAI, K.[1]; TANIGUCHI, H.[3]**
*([1]Hokkaido Univ.; [2]IMS and Hokkaido Univ.; [3]Saitama Univ.)*

Quasi-two-dimensional (Q2D) organic conductor (BEDT-TTF)$_3$Cl$_2$·2H$_2$O is metallic at 300 K and it undergoes metal–insulator transition (MIT) at $T$ ~ 150 K from magnetic susceptibility and electric conductivity measurements. The MIT has been believed to be connected with charge density wave (CDW) formation. However, the formation of the charge ordering (CO) in the insulator phase was also expected. Using $^{13}$C-NMR measurement, we observed the split of the NMR spectrum which corresponded to the charge rich and poor sites below the MIT temperature and could conclude the insulator state is in the CO state.

From electric conductivity measurement under pressures for this compound, it is found that the metal–insulator transition is suppressed by applying pressure and this compound shows superconductivity above 1.6 GPa. In order to inspect how CO state formed under ambient pressure is changed, we measured $T_1$ under pressures. Regrettably, we could get no information from NMR spectrum because of the broadening spectrum due to magnetism of the pressure cell. Below 1.4 GPa, we observed $(T_1T)^{-1}$ = constant at high temperature and decreased at low temperature, just same as ambient pressure. This indicates that the formation of the gap $\Delta$ also exists under pressures. As we have done above, we estimated the gap $\Delta$ at each pressure by means of thermal activation model fitting. We could confirm the existence of the gap $\Delta$ until 1.4 GPa. Both the gap $\Delta$ and $T_g$ decreased with increasing pressure until 1.4 GPa. By applying pressure, transfer integral $t$ in conductivity chain increases and enhance itinerant-electron system. As the results, the amplitude of the charge dispropotionation becomes small and the gap $\Delta$ is decreasing. In addition, as compared to metal–insulator transition temperature $T_{\mathrm{MI}}$ estimated from electric conductivity measurement, $T_g$ behaves in a way similar to $T_{\mathrm{MI}}$, just as ambient pressure. We predict that a strong correlation between two temperatures; $T_g$ and $T_{\mathrm{MI}}$, exists.With decreasing temperature, $(T_1T)^{-1}$ shows almost constant like a metallic behavior. This indicates that the system changes an itinerant-electron system and the localization of the carrier by CO vanishes. It is important for the elucidation of the mechanism of superconductivity to consider whether the system is a simple metallic state or an exotic metallic state in which itinerant-electron system and charge disproportionation coexist.

## IV-E-2 $^{13}$C-NMR Study of Single Crystal of β'-(BEDT-TTF)(TCNQ) under Pressure

**ETO, Y.[1]; OGURA, T.[1]; KAWAMOTO, Atsushi[2]; KUMAGAI, K.[1]; YAMAMOTO, Kaoru; YAKUSHI, Kyuya**
*([1]Hokkaido Univ.; [2]IMS and Hokkaido Univ.)*

Organic conductor β'-(BEDT-TTF)(TCNQ) is the material in which BEDT-TTF molecules form two-dimensional structure and TCNQ molecules form one-dimensional stacked structure, and both molecules are in the form of dimer. Properties of this salt shows metal insulator transition (M–I transition) at 330 K at ambient pressure, and transition temperatures decrease by applying pressure. It is known that BEDT-TTF molecule and TCNQ molecule show different magnetic properties so that an antiferromagnetic ordering occurs in the former at 20 K and the latter occurs at 3 K. In addition, properties of this salt under pressure are interested very much from the point of view that the layer structure of BEDT-TTF have the same type of structure of β'-(BEDT-TTF)$_2$ICl$_2$ which has the highest $T_{\mathrm{C}}$ under pressure among the organic conductors. So we performed $^{13}$C-NMR measurements using single crystal of (BEDT-TTF)(TCNQ) where one site of the central double-bonded carbon in BEDT-TTF molecule is labeled by $^{13}$C. BEDT-TTF forms a dimer in a layer. It is expected that two peaks are observed in the high temperature. Actually, two peaks were seen in the observed spectrum in the high temperature side. We can estimate a local susceptibility only for a BEDT-TTF site by using NMR at selected site. One peak was observed in the vicinity of almost knight shift 0 at antiferromagnetic transition temperature (20 K) and understood that line width increased as lowering temperature. We measured in a range of ±1 MHz at 10 K, but the other peaks were not observed. It suggests that antiferromagnetic transition of this material is not commensurate but incommensurate. We are also going to report about the result of under pressure.